Plasmons in tunneling coupled bilayer systems with tunable space symmetry studied by far-infrared spectroscopy

S. Holland, C.-M. Hu, Ch. Heyn, and D. Heitmann
Institut für Angewandte Physik, Jungiusstrasse 11, D-20355 Hamburg, Germany
(Received 28 March 2002; published 15 August 2002)

Tunneling coupled bilayer systems based on $Al_{0.33}Ga_{0.67}As/GaAs$ heterostructures have been investigated with far-infrared spectroscopy (FIR) and magnetotransport measurements. Via a Ti front gate the charge density as well as space symmetry of the bilayer are tuned. Using FIR spectroscopy we observe intrasubband optical plasmon modes and an intersubband plasmon. From magnetotransport measurements we determine the single-particle tunneling gap Δ_{SAS} between the symmetric and antisymmetric subband. By comparing Δ_{SAS} with the resonance energy of the intersubband plasmon, we are able to determine directly from measurement the depolarization shift, i.e., a many-body correction to the intersubband excitation. We study its behavior by changing the space symmetry of the bilayer system.

DOI: 10.1103/PhysRevB.66.073305 PACS number(s): 73.20.Mf, 71.45.Gm, 73.21.Fg

Bilayer systems with two two-dimensional electron gases (2DEG's) separated by a barrier with a width at the order of tens of nanometers have been long interested due to their rich many-body effects. Das Sarma *et al.*[1] predicted twenty years ago the existence of an undamped acoustic plasmon with a linear q dispersion in addition to an optical plasmon with a $\sqrt{q}$ dispersion in a Coulomb coupled double quantum well system. In the optical (acoustic) plasmon mode the charge densities of the layers oscillate in (out of) phase. These modes were observed in Raman experiments.[2] Reducing the barrier to the order of a few nanometers, tunneling effects between the two 2DEG's become significant. Theoretical understanding of the plasmons in such tunneling-coupled bilayer systems is currently under discussion.[3–7] Systematic experimental study are highly needed to investigate the influences of tunneling on plasmon modes.

From the experimental point of view, an elegant way of changing tunneling behavior is to use the gated bilayer system. By applying a gate voltage across two quantum wells separated by a thin barrier where the bilayer 2DEG's are formed, the energy levels in each quantum well shift, changing the way of the wave function mixture induced by tunneling.[8] Here the tunneling effect is tuned by varying the space symmetry of the two quantum wells instead of changing the tunneling matrix element that requires changing the sample structure. When the two quantum wells are symmetrically aligned, the energy states of the bilayer system are tunneling mixed delocalized states. The lowest subband splits into a symmetric $|S\rangle$ and an antisymmetric state $|AS\rangle$ with an energy gap Δ_{SAS}. When the two quantum wells become more and more asymmetric, $|S\rangle$ and $|AS\rangle$ states get more and more localized in different quantum wells with an increasing energy gap Δ between the two states. Tunneling effect becomes negligible if $\Delta \gg \Delta_{SAS}$. Our recent theoretical study[7] shows that at least three different plasmon modes exsisting in a tunneling-coupled bilayer system, namely, the intrasubband optical and acoustic plasmons, and an intersubband plasmon (ISP) that can also be understood as the depolarization shifted intersubband resonance.[9–11]

In this paper we report the observation of plasmon modes in tunneling coupled bilayer systems by using far-infrared (FIR) spectroscopy. We focus on the gate-voltage dependence of the mode energies. By comparing the ISP energy measured by FIR spectroscopy with the single-particle intersubband energy gap Δ obtained by magnetotransport measurements, we are able to determine directly the depolarization shift, i.e., a many-body correction to the intersubband resonance.

Our samples were grown with molecular beam epitaxy and have the following layer structure: a 280 nm AlAs/GaAs superlattice (period: 5.6 nm), a buffer of 500 nm GaAs and 250 nm $Al_{0.33}Ga_{0.67}As$ and a Si δ-donor layer. The bilayer structure which is grown on top consists of 30 nm $Al_{0.33}Ga_{0.67}As$, 15 nm GaAs, 1 nm $Al_{0.33}Ga_{0.67}As$, 15 nm GaAs, and 20 nm $Al_{0.33}Ga_{0.67}As$. It is followed by a Si δ-donor layer, 10 nm $Al_{0.33}Ga_{0.67}As$, a Si δ donor layer, 10 nm $Al_{0.33}Ga_{0.67}As$ and a 5 nm GaAs cap layer.

After preparing a macro Hall-bar mesa with a width of 3 mm, Ohmic contacts were made by depositing Au-Ge followed by annealing. A 8 nm Ti front gate was then evaporated onto the sample. On top of the gate we fabricated an Au grating coupler with a period of $a=2$ μm. The grating coupler selects wave vectors for the optical plasmon modes with $q_n = n(2\pi/a)$, $n=1,2,\ldots$. The excitation strength of these modes becomes weaker for higher index n. The grating also couples FIR light to intersubband plasmon via the optical near-field components with electric fields perpendicular to the 2DEG's plane.

The FIR measurements were performed using a Fourier transform spectrometer which is connected to a 12 T superconducting magnet via a wave-guide system. Spectra were taken at different gate voltages V_g and are normalized with that measured at the threshold voltage $V_{\mathrm{th}} = -1.2$ V. The result is the relative change $T(V_g)/T(V_{\mathrm{th}})$. Magnetotransport measurements at the same gate voltages were carried out *in situ* by applying the magnetic field up to 12 T. The sample temperature was 2.2 K at all times.

Figure 1 shows the measured spectra at three different gate voltages. For a better overview they are vertically shifted. Up to four resonances can be seen. By analyzing the gate-voltage dependence of the resonance energies, the

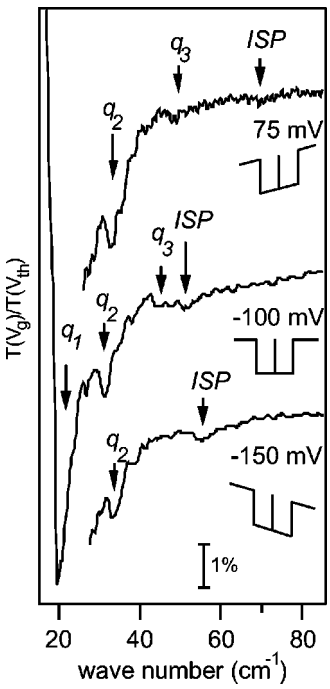

FIG. 1. Experimental plasmon excitations observed in a front-gated $Al_xGa_{1-x}As/GaAs$ bilayer heterostructure. The gate voltages 75, -100, and -150 mV correspond to a total charge density of 7.58, 6.06, and 5.43×10^{11} cm^{-1}, respectively. The resonances denoted with $q_n, n=1,2,3$ are optical plasmon modes, the intersubband plasmon is labeled with ISP. The space symmetry of the bilayer system is shown schematically at different gate voltages.

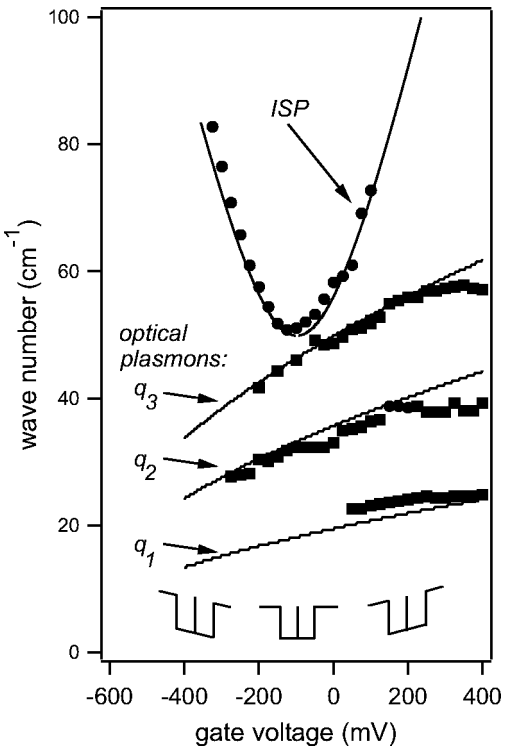

FIG. 2. Measured (marks) and calculated (lines) gate-voltage dispersion of plasmon modes. The optical plasmon mode energies (■) increase monotonically with increasing gate voltage, i.e., charge density. The ISP mode energy (●) is governed by the space symmetry of the bilayer structure.

modes labeled with q_1, q_3, and q_3 are identified as intrasubband optical plasmons with the corresponding wave vectors q_n. It is clearly seen that the oscillator strength decreases for higher wave vectors, i.e., higher index numbers n. The mode with the highest energy is identified as the intersubband plasmon corresponds to intersubband transitions between the tunneling split subbands $|S\rangle$ and $|AS\rangle$. When the bilayer system is tuned to be asymmetric the resonance shifts to significantly higher energies. Because of the low sensitivity of the spectrometer at wave numbers smaller than 20 cm^{-1} the intrasubband acoustic plasmon which should exist below the intrasubband optical plasmon mode cannot be observed.

The gate-voltage dependence of the plasmon mode energies is shown in Fig. 2. Intrasubband optical plasmon mode is described by the following relation,[12] neglecting the nonlocal corrections

$$\omega_p = \sqrt{\frac{N_s e^2 q}{2\epsilon_0 \epsilon^* m^*}}. \tag{1}$$

Here N_s is the total carrier density, q the wave vector, m^* the effective mass, and ϵ^* an effective dielectric constant.

The presence of a gate in the direct proximity of the 2DEG changes the dielectric constant for plasmons propagating parallel to the 2DEG.[13] Therefore an effective dielectric constant with the form

$$\epsilon^* = \epsilon_{\mathrm{GaAs}}(1+\coth q d_{\mathrm{gate}}). \tag{2}$$

is introduced, which is now dependent on the wave vector q, the distance d_{gate} between the 2DEG and the gate, and the dielectric constant of the $Al_xGa_{1-x}As$ layer in between. We assume an identical value of the dielectric constant for $Al_xGa_{1-x}As$ and GaAs of $\epsilon_{\mathrm{GaAs}}=12.8$. We have $d_{\mathrm{gate}}=55$ nm. We determine $m^*=0.07m_e$ by cyclotron resonance experiment.

From Fourier transformation of the Shubnikov–de Haas oscillations measured by magnetotransport experiment we determine the gate voltage dependent density as shown in the inset of Fig. 3. The total carrier density is found of a linear dependence on the gate voltage up to 200 mV. At higher values it saturates because of increasing leakage currents. Using the linear gate-voltage dependence of the carrier density, we calculate the gate-voltage dispersions of the optical plasmons and show them in Fig. 2. The calculated dispersions for optical plasmon modes with wave vectors q_2 and q_3 agree well with that measured. The agreement between theory and experiment for the q_1 mode is less satisfactory mainly due to the increasing difficulty in determining the experimental resonance position at wave numbers below 20 cm^{-1}.

In contrast to the optical plasmons the measured ISP resonance position does not increase monotonically with increasing gate voltage, i.e., charge density but is strongly dependent on the space symmetry. To analyze the ISP mode we use our recent developed theory on plasmons in tunneling coupled bilayer systems.[7] We set the parameter $d=16$ nm

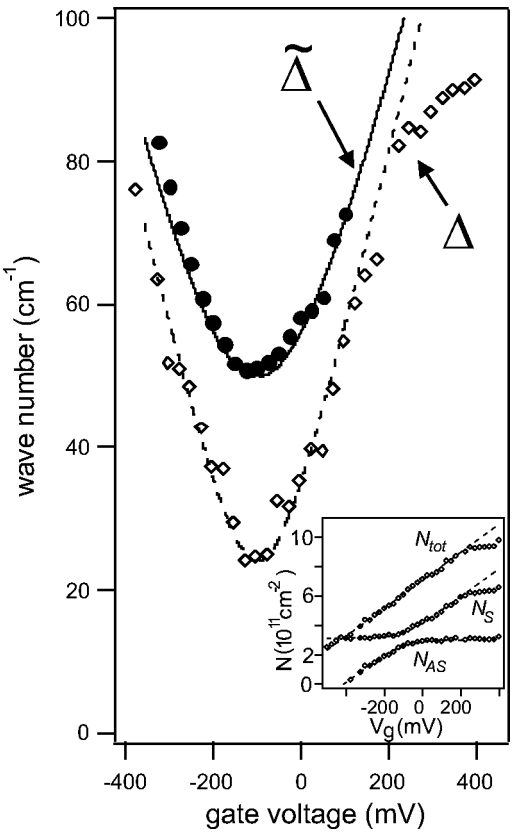

FIG. 3. Measured gate-voltage dependence of intersubband excitation energy $\tilde{\Delta}$ (●) and the single-particle gap Δ (◇). The line is calculated using a theory for plasmon in Ref. 7. The dashed lines are guide to eyes. The insert shows the gate-voltage dependence of the charge density $N_{S/AS}$ of the symmetrical/antisymmetrical subband and the total charge density N_{tot}.

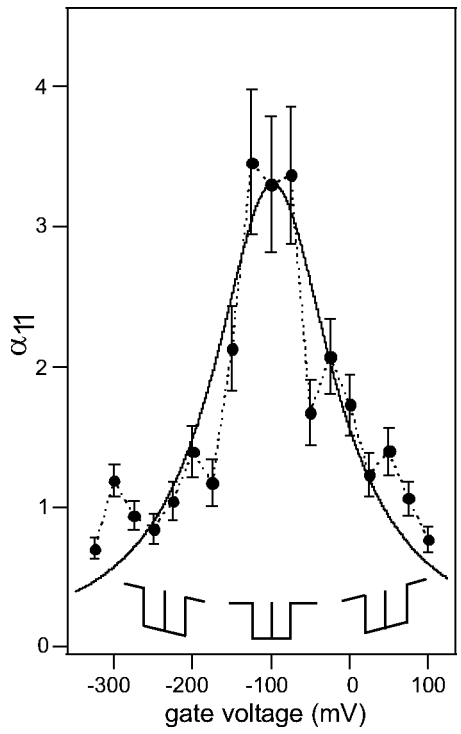

FIG. 4. Experimental and theorical depolarization shift α_{11}. The space symmetry of the bilayer system is shown schematically for different gate-voltage ranges.

that is the distance between the center of the quantum wells and determine the tunneling gap in the symmetrical case $\Delta_{SAS}=3$ meV by magnetotransport measurement. In the case of an ISP the charges oscillates perpendicular to the 2DEG's. The variation of the spatial charge distribution in growth direction is very small (a few nanometers) in contrast to that for optical or acoustic plasmons which is in the order of the grating coupler dimensions. The electrical fields associated with the ISP are less influenced by the gate. We use a value of the dielectric constant of $\epsilon=12.8$ that is the bulk value for GaAs. Our results explain the approximately parabolic gate-voltage dispersion of ISP mode and show that the space symmetry has a strong influence on it.

It is also interesting to compare the ISP mode energy with the single-particle intersubband energy Δ since the ISP mode can be viewed as an intersubband excitation influenced by the depolarization shift. If both the $|S\rangle$ and $|AS\rangle$ states are populated, Δ can be determined by the relation

$$\Delta=\frac{N_S-N_{AS}}{D_2}, \tag{3}$$

in which $D_2=m^*/\pi\hbar^2$ is the two-dimensional density of states, N_S and N_{AS}, respectively, are the charge densities of the symmetric and the antisymmetric subband, that can be measured from Shubnikov–de Haas oscillations. Here we neglect a small many-body correction to Δ[14] that is less than 4% and lies within the measurement error of our results. Figure 3 shows comparatively the gate-voltage dependence of the intersubband excitation energy $\tilde{\Delta}$ and the intersubband energy Δ measured by FIR spectroscopy and magnetotransport, respectively. Dashed lines across the open marks are guides to the eyes. Lines across the solid marks are the calculated ISP modes energy based on the theory in Ref. 7. In a first moment it is surprising that, in spite of an increasing total density, the depolarization shift decreases for $V_g> -100$ mV. One reason is that due to the occupation of the antisymmetric subband final states are blocked. In a simple picture when Δ does not depend on the gate voltage this would lead to a constant depolarization shift. The reason for the decrease is more subtile.

Note that our theory in the frame work of plasmon excitations already explains well the overall enhancements of the ISP mode energy compared with the intersubband excitation energy Δ. In the following we provide an alternative analysis using the formalism of depolarization-shifted intersubband resonance to elucidate the behavior of the depolarization shift.[9,15]

The depolarization shifted intersubband resonance $\tilde{\Delta}$ is given by

$$\tilde{\Delta}=\Delta\sqrt{1+\alpha_{11}}, \tag{4}$$

where the depolarization shift α_{11} is (Ref. 15)

$$\alpha_{11}=\frac{2e^2}{\epsilon_\infty\epsilon_0}\frac{N_S-N_{AS}}{\Delta}L_{11}, \tag{5}$$

with L_{11} the Coulomb length tensor

$$L_{11}=\int_{-\infty}^{\infty}dz\left(\int_{\infty}^{z}dz'\chi_1(z')\chi_0(z')\right)^2. \tag{6}$$

We can safely neglect the so called exciton shift because the total charge density is large in our sample.[9] To calculate α_{11} we use the pseudospin formalism[7,8,16]. The wave functions in space coordinates are $\chi_0(z)=\delta(z+d/2)\sin(\Theta/2)+\delta(z-d/2)\cos(\Theta/2)$ and $\chi_1(z)=\delta(z+d/2)\cos(\Theta/2)-\delta(z-d/2)\sin(\Theta/2)$ with $\sin\Theta=\Delta_{SAS}/\Delta$, $\delta(Z)$ the Dirac delta function and $d=16$ nm is the distance between the center of the two layers. The integral is easily calculated:

$$L_{11}=\frac{d}{4}\sin^2\Theta. \tag{7}$$

We find therefore the depolarization shift α_{11} has the form of

$$\alpha_{11}=\frac{2e^2D_2}{\epsilon_\infty\epsilon_0}\frac{d}{4}\sin^2\Theta, \tag{8}$$

depending on the parameter $\sin\Theta$ that describes the space symmetry of the bilayer system.[7] So we can see directly that the depolarization shift exhibits a maximum in the symmetric case ($\sin\Theta=1$) and then decreases in spite of the increasing density due to the increasing asymmetry. Using Eq. (8) together with the transport measured gate-voltage dependence of the intersubband energy Δ, we plot in Fig. 4 with a solid line the predicted depolarization shift α_{11} as a function of the gate voltage. On the other hand α_{11} can be directly determined from Eq. (4) using the FIR measured data of $\tilde{\Delta}$ and the transport measured Δ. These we plot in Fig. 4 with circles. Our calculated curve lies within the tolerance of the experimental results. The measurement error results mainly of the inaccuracy of the determination of the charge densities.

In conclusion, we have prepared a $Al_xGa_{1-x}As/GaAs$ based bilayer heterostructure with a front gate, ohmic contacts and a 2 μm grating coupler. With FIR spectroscopy we observe up to three optical plasmon modes and the intersubband excitation $|S\rangle\rightarrow|AS\rangle$. With magnetotransport we determined the single-particle energy gap Δ. The depolarization shift is determined by comparing the energy of the intersubband excitation $\tilde{\Delta}$ and the single-particle energy gap Δ and agrees well with the theory. Space symmetry strongly influences the depolarization shift.

This work was financially supported by the NEDO International Joint Research Grant, the BMBF through Project No. 01BM905 and the DFG through Grant No. SFB 508.

[1] S. Sarma and A. Madhukar, Phys. Rev. B **23**, 805 (1981).
[2] G. Fasol, N. Mestres, H. Hughes, A. Fischer, and K. Ploog, Phys. Rev. Lett. **56**, 2517 (1986).
[3] S. Sarma and E. Hwang, Phys. Rev. Lett. **81**, 4216 (1998).
[4] P.G. Bolcatto and C. Proetto, Phys. Rev. Lett. **85**, 1734 (2000).
[5] P.G. Bolcatto and C. Proetto, Phys. Rev. Lett. **85**, 679 (2000).
[6] S. Sarma and E. Hwang, Phys. Rev. Lett. **85**, 680 (2000).
[7] C.-M. Hu, C. Schüller, and D. Heitmann, Phys. Rev. B **64**, 073303 (2001).
[8] C.-M. Hu and D. Heitmann, Appl. Phys. Lett. **77**, 1475 (2000).
[9] T. Ando, A.B. Fowler, and F. Stern, Rev. Mod. Phys. **54**, 437 (1982).
[10] S. Graf, H. Sigg, K. Köhler, and W. Bächtold, Phys. Rev. Lett. **84**, 2686 (2000).
[11] P. Denk, M. Hartung, A. Wixforth, K. Campmann, and A. Gossard, Physica E (Amsterdam) **8**, 269 (2000).
[12] F. Stern, Phys. Rev. Lett. **18**, 546 (1967).
[13] T.N. Theis, Surf. Sci. **98**, 515 (1980).
[14] L. Swierkowski and A. Macdonald, Phys. Rev. B **55**, R16 017 (1997).
[15] M. Zaluzny, J. Appl. Phys. **74**, 4716 (1993).
[16] T. Jungwirth and A. Macdonald, Phys. Rev. B **53**, 9943 (1996).